Food and Chemical Toxicology 141 (2020) 111394

Contents lists available at ScienceDirect

Food and Chemical Toxicology

journal homepage: www.elsevier.com/locate/foodchemtox

(-)-Syringaresinol-4-O-β-D-glucopyranoside from Cortex *Albizziae* inhibits corticosterone-induced PC12 cell apoptosis and relieves the associated dysfunction

Desen Yang[a,b], Wanqin Wu[d,e], Guoping Gan[b,c], Dingkun Wang[a], Jing Gong[a], Ke Fang[a], Fuer Lu[a,*]

[a] Institute of Integrated Traditional Chinese and Western Medicine, Tongji Hospital, Tongji Medical College, Huazhong University of Science and Technology, 1037 Jiefang Road, Qiaokou District, Wuhan, 430030, Hubei Province, China
[b] College of Pharmacy, Hubei University of Chinese Medicine, 16 Huangjiahu West Road, Hongshan District, Wuhan, 430065, Hubei Province, China
[c] Chinese Materia Medica Processing Engineering Center of Hubei Province, Hubei University of Chinese Medicine, 16 Huangjiahu West Road, Hongshan District, Wuhan, 430065, Hubei Province, China
[d] Hubei Provincial Institute for Food Supervision and Test, 1 Gaoxin Road, Jiangxia District, Wuhan, 430070, Hubei Province, China
[e] Hubei Provincial Engineering and Technology Research Center for Food Quality and Safety Test, 1 Gaoxin Road, Jiangxia District, Wuhan, 430070, Hubei Province, China

ARTICLE INFO

Keywords:
(-)-Syringaresinol-4-O-β-D-glucopyranoside
Corticosterone
PC12 cell
Antiapoptotic effect
Neuroprotective effect
Anxiolytic

ABSTRACT

The neuroprotective effects and potential mechanisms of (-)-Syringaresinol-4-O-β-D-glucopyranoside (SRG), a natural lignan glycoside extracted from Cortex *Albizziae*, were investigated using corticosterone (CORT)-induced PC12 cells as an in vitro anxiety model. PC12 cells were treated with 100 μM CORT and 5, 10, or 20 μM SRG for 48 h. Cell viability and lactate dehydrogenase (LDH) leakage were measured. Apoptosis were detected using FITC-coupled Annexin V (AV) and propidium iodide (PI) staining flow cytometric analyses and TUNEL assays. Rhodamine 123 and Fluo-3-AM staining flow cytometric analyses were used to detect mitochondrial membrane potential (ΔΨm) and intracellular calcium concentration ($[Ca^{2+}]_i$), respectively. Western blot was used to detect brain-derived neurotrophic factor (BDNF), Bax, Bcl-2, cAMP-response element binding protein (CREB), cytosolic cytochrome *c* (Cyt *c*), caspase-3, and cleaved caspase-3. Experimental data showed that SRG promoted cell proliferation, reduced LDH release, inhibited apoptosis, improved ΔΨm values, decreased $[Ca^{2+}]_i$, up-regulated CREB, BDNF, and Bcl-2, down-regulated Bax and Cyt *c* protein expression levels, and reduced caspase-3 activity. This suggests that SRG has neuroprotective and antiapoptotic effects in the pathogenesis of anxiety disorders, and its mechanisms are partly connecte to inhibition of the mitochondrial apoptotic pathway and activation of pathways involving CREB and BDNF.

1. Introduction

Anxiety is a physiological and psychological disease with high incidence that seriously affects quality of life (Elhai et al., 2018; Zhang et al., 2018; Schaefer et al., 2018). At present, drug therapy is considered an important anxiety treatment. Although sufficient to relieve symptoms, all currently available drugs have obvious drawbacks. Use of these medications can result in abuse or dependence, retrograde amnesia (benzodiazepines), delayed clinical efficacy (bupropion and antidepressants), sexual dysfunction (antidepressants), sedation (benzodiazepines and pregabalin), and vertigo (pregabalin), all of which affect clinical compliance (Nash and Nutt, 2005; Lader and Morton, 1991). These limitations highlight the necessary and urgent development of new anti-anxiety drugs. Recently, various herbal medicines have been used as alternative anti-anxiety remedies (Carlini, 2003).

Cortex *Albizziae*, the stem bark of the leguminous plant, *Albizzia julibrissin* Durazz, is a widely used traditional Chinese medicine with a tranquilizing effect (Yu et al., 2004; Tong et al., 2003; Zheng et al., 2004). However, the tranquilizing active ingredients and mechanisms of Cortex *Albizziae* remain unclear. Some studies have suggested that aqueous Cortex *Albizziae* extract has anxiolytic-like activity in animal models (Kim et al., 2004; Jung et al., 2005, 2013bib_Jung_et_al_2005bib_Jung_et_al_2013; Liu et al., 2017). Our preliminary study showed that one of the aqueous Cortex *Albizziae* extracts, which we referred to as s-75, had significant anti-

* Corresponding author.
E-mail addresses: yds22@126.com (D. Yang), 429371379@qq.com (W. Wu), 510577319@qq.com (G. Gan), wdkung@163.com (D. Wang), 983764792@qq.com (J. Gong), 370440692@qq.com (K. Fang), 176526492@qq.com (F. Lu).

https://doi.org/10.1016/j.fct.2020.111394
Received 12 January 2020; Received in revised form 22 April 2020; Accepted 24 April 2020
Available online 30 April 2020

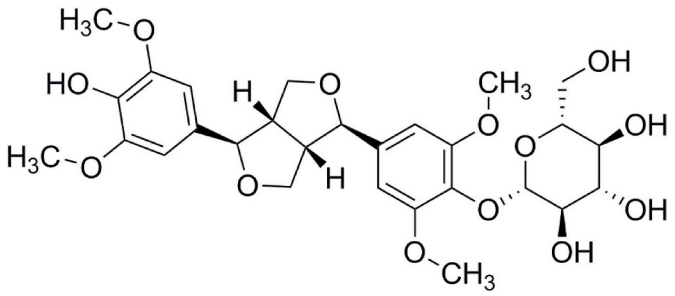

Fig. 1. Chemical structure of (-)-Syringaresinol-4-*O*-β-D-glucopyranoside (SRG).

anxiety properties as evaluated by open field test, light and dark test, and elevated maze test (Tian, 2015). Then, we found that (-)-Syringaresinol-4-O-β-D-glucopyranoside (SRG) was just one of the main component of s-75 (Fan, 2016), Fig. 1 depicts the structure of SRG, we speculated that it might be one of the main active tranquilizing components of Cortex *Albizziae*.

Studies have shown that the occurrence of anxiety and other mental disorders might be related to hyperfunction of the hypothalamic-pituitary-adrenal (HPA) axis and damage caused by excessive glucocorticoid including corticosterone (CORT), a principal glucocorticoid, delivered to the hippocampus and other brain nerve tissues (Battaglia and Ogliari, 2005; Seckl and Meaney, 2004; Zhu, M.Y. et al., 2006; Zhu, Z.H. et al., 2006). The differentiated PC12 cell line cloned from rat chromophage cells possesses typical nerve cell characteristics and expresses high levels of glucocorticoid receptors, which can combine with CORT (Anderson and Michelsohn, 1989). This feature enables PC12 cells damaged by CORT to simulate the central nervous system injury state in anxiety disorder and to be reversed by treatment with an anti-anxiety agent (Li et al., 2002, 2003, 2004bib_Li_et_al_2002bib_Li_et_al_2003bib_Li_et_al_2004). Further studies have found that apoptosis might be the main form of CORT-induced neuron injury (Jiang et al., 2014; Li et al., 2016).

The cAMP-response element binding protein (CREB)-brain-derived neurotrophic factor (BDNF) pathway plays an important role in emotional disorders (Ji et al., 2017; Li et al., 2017). Activated CREB could promote the differentiation of nerve cells, increase synaptic plasticity and nerve regeneration by increasing BDNF protein expression (Lonze and Ginty, 2002; Mohammadi et al., 2018). BDNF, as the most studied neurotrophic factor in anxiety disorder, is believed to be related to the cellular mechanism and neuroplasticity of CREB (Hempstead, 2015; Levada and Cherednichenko, 2015; Duman, 2017). Current research suggests that BDNF is involved in posttraumatic anxiety (Andero and Ressler, 2012; Bennett et al., 2016). An anxiolytic could increase CREB and BDNF expression in the rat hippocampus (Yu et al., 2015; Antipova et al., 2009; Li et al., 2010). It was reported that BDNF was expected to inhibit apoptosis by increasing the expression of bcl-2 protein, a key factor in mitochondrial stress-induced apoptosis (Sun et al., 2012). There has been growing evidence that BDNF influences apoptosis through mitochondrial pathways (Lang et al., 2007; Peng et al., 2008).

Here, we constructed an in vitro anxiety model through CORT-induced PC12 cells damage to explore the neuroprotective activity and the underlying mechanisms of the effect of SRG. These findings will lay a good foundation for further research on the anti-anxiety effect of SRG and will help develop novel anxiolytic targeting CREB-BDNF and mitochondrial apoptosis pathways.

2. Methods and materials

2.1. Chemicals and reagents

SRG (ChemBlink CAS Registry Number: 137038-13-2) ((purity exceeding 98%, Fig. S1 (supplementary materials)) was obtained from Chengdu Biopurify Phytochemicals Ltd. (BP3135, Chengdu, Sichuan Province, China). Buspirone (BUS) was obtained from Selleck (S4256, Houston, TX, USA). CORT (B1509002) was obtained from Aladdin (Shanghai, China). Gibco (Grand Island, NY, USA) provided Trypsin (15050065) and RPMI 1640 Medium (72400120). Penicillin and streptomycin mixed solution (DY14011), FBS (SV30087.02), and horse serum (DY14011) were obtained from Hyclone (Logan City, UT, USA). Dimethyl sulfoxide (DMSO) (D2650), Sigma (St. Louis, MO, USA) provided nerve growth factor-7S (NGF-7S) (N0513), MTT (C0009-2), and Rhodamine 123 detection kit (R8004). Beyotime Institute of Biotechnology (Shanghai, China) provided Triton X-100 (ST795), DAPI (C1002), Fluo-3-methyl acetyl (AM) Ca^{2+} Concentration detection kit (S1056), phenylmethylsulphonyl fluoride (PMSF) (ST506), RIPA lysis buffer (P0013B), and BCA Protein Colorimetric Assay kit (P0010). Nanjing Jian Cheng Bioengineering Institute (Nanjing, Jiangsu Province, China) provided Lactate dehydrogenase (LDH) detection kit (A020-2). Nanjing KeyGen Biotech (Nanjing, Jiangsu Province, China) provided FITC-Annexin V (AV) and propidium iodide (PI) apoptosis detection kit (KGA108). TUNEL Cell Apoptosis Detection kits (12156792910) were purchased from Roche Applied Science (Indianapolis, IN, USA). N,N,N′,N′-Tetramethylethylenediamine (Amresc00761), Tris-base (Exp2017/12), bromophenol blue (BO449-5G), acrylamide (Exp2016109), and methacrylamide (Amresc00172) were obtained from AMRESCO (Solon, TX, USA). Paraformaldehyde (4%; 80096618) and SDS (30166428) were purchased from China Pharmaceutical Group (Shanghai, China), and TBST buffer (E-BC-R335) was obtained from Elabscience Biotechnology Co., Ltd (Wuhan, Hubei Province, China).

2.2. Cell culture

The PC12 cells required for this experiment were provided by Cell Bank of Shanghai institute of life sciences (SCSP-517, Chinese Academy of Sciences, Shanghai, China). PC12 cells solution was prepared by adding 5% horse serum (inactivated by heat) and penicillin and streptomycin mixed solution into RPMI 1640 Medium. The cells were then placed in a CI-080-A CO_2 incubator (SANYO, Osaka, Japan) at an ambient temperature of 37 °C. First, we added NGF-7S (50 ng/mL) to PC12 cell fluid, and NGF-7S induced PC12 cells to become differentiated exponential PC12 cells, which grew nerve fibers (Dobashi et al., 1996). Next, experiments were conducted using differentiated exponential cells. In our previous study, we discovered that PC12 cells were markedly damaged after being treated with 100 μM CORT for 48 h (Fig. S2 (supplementary materials)). Therefore, this concentration was employed in this study. The treated cells were grouped as follows: control (the cell culture medium was not changed); 100 μM CORT; 100 μM CORT and either 10 μM BUS or 5, 10, or 20 μM SRG, respectively.

2.3. Cell viability

Succinic acid dehydrogenase in the mitochondria of living cells reduces MTT to a blue-violet crystal (Formazan), but dead cells have no such function. Therefore, we used the MTT assay to determine cell viability (Du et al., 2018). PC12 cells (5×10^4 cells/mL) at logarithmic growth stage were inoculated in the cell culture plate, each well containing 100 μL cell suspension. Cell grouping and treatment were described in the Cell culture subsection. Next, the cells were cultured for 4 h after we added 10 μL MTT to each well. Then, 150 μL DMSO (Formazan solvent) was used to replace medium containing MTT for a 10-min stimulation period. The OD value (568 nm) of each well was determined with a MK3 Microplate Reader (Thermo Fisher Scientific, Waltham, Massachusetts, USA). The calculation results were as follows:

$$\text{Cell viability (\%)} = \frac{\text{OD(treated group)} - \text{OD(blank control without cells)}}{\text{OD(non - treated control group)} - \text{OD(blank control without cells)}} \times 100 \quad (1)$$

2.4. Lactate dehydrogenase (LDH) assay

When the cell membrane is damaged, LDH is released to the outside of the cell. Therefore, the extent of cell damage can be determined by colorimetric determination of LDH in the medium (Du et al., 2018). The cells were lysed and the supernatant was harvested after treatment. Total activity colorimetry for LDH in the supernatant was determined in strict accordance with the instructions of the LDH detection kit. The OD value (450 nm) of the reaction mixture was determined with a MK3 Microplate Reader. The results were calculated using the following formula:

$$\text{LDH activity (U/L)} = \frac{\text{OD(sample hole)} - \text{OD(control hole)}}{\text{OD(standard hole)} - \text{OD(blank hole)}} \times 200 \times \text{dilution multiple of sample} \quad (2)$$

2.5. Flow cytometry analysis

AV (Ca^{2+}-dependent phospholipid binding proteins) may be used to label phosphatidylserine exposed by membrane specific valgus in the early stage of apoptosis. PI (nucleic acid dye) can permeate cell membrane and dye the nucleus red in the later stage of apoptosis. Flow cytometry can detect apoptosis in cells labeled with AV and PI (Cheng et al., 2018). This experiment was performed in strict accordance with the instructions of FITC-AV and PI apoptosis Assay kit. Briefly, and then analyzed by a Cytomics™ FC 500 MCL flow cytometry (Beckman Coulter, Indianapolis, IN, USA).

2.6. TUNEL assay analysis

In the late stage of apoptosis, under the action of terminal deoxyribonucleotide transferase, deoxyribonucleotide-luciferin (red fluorescence) conjugate labels the 3′-end of the DNA gap, and the labeled DNA can be directly observed by fluorescence microscopy (Mohammad Alizadeh et al., 2018). The cells were grown on slides after treatment, and then this experiment was performed in strict accordance with the instructions of TUNEL Cell Apoptosis Detection kits. Finally, the images of slides were observed and collected under a BX53 fluorescence inverted microscope (Olympus Corporation, Tokyo, Japan).

2.7. Measurements of mitochondrial membrane potential ($\Delta\Psi m$)

Rhodamine 123 is a cationic fluorescent dye that can penetrate the cell membrane. In normal cells, it can enter the mitochondrial matrix depending on the mitochondrial transmembrane potential, where its fluorescence intensity is weakened or disappears. During apoptosis, the mitochondrial permeability transition pore opens and $\Delta\Psi m$ collapses. Rhodamine 123 is then released from the mitochondria, producing a strong yellow-green fluorescence (Yin et al., 2009). This experiment was performed in strict accordance with the instructions of Rhodamine 123 detection kit. PC12 cells were incubated with 10 mg/L Rhodamine 123 in a CI-080-A CO_2 incubator at an ambient temperature of 37 °C for 45 min away from light after treatment, then analyzed using a Cytomics™ FC 500 MCL flow cytometer. The changes in $\Delta\Psi m$ and apoptosis were detected by yellow-green fluorescence signal intensity.

2.8. Measurements of intracellular Ca^{2+} concentration ($[Ca^{2+}]_i$)

Fluo-3 (calcium ion flow fluorescent probe) itself can not penetrate the cytoplasmic membrane into the cell. When it is linked to AM, it can be introduced into cells, hydrolyzed by intracellular nonspecific esterase, and restored to the form of free acids that bind to intracellular calcium. Calcium ion concentration can be detected sensitively by its fluorescence intensity (Seo et al., 2016). This experiment was performed in strict accordance with the instructions of Fluo-3-AM Ca^{2+} concentration detection kit, and then analyzed by a Cytomics™ FC 500 MCL flow cytometer.

2.9. Western blot

RIPA lysis buffer (containing 100 mM PMSF) was used to obtain total PC12 cell proteins after treatment. Then, the protein contents of total PC12 cell were measured in strict accordance with the instructions of BCA protein detection kit. Proteins (40 μg) were split by SDS-PAGE and moved to PVDF membranes (0.45 μm (IPVH00010) and 0.22 μm (ISEQ15150), Millipore Corporation, Bedford, MA, USA). The membranes were soaked in TBST buffer with 5% skim milk for 2 h, then soaked in TBST buffer overnight with corresponding antibodies: anti-CREB (ab32515 1:1000), anti-BDNF (ab108319, 1:2000), anti-Bcl-2 (ab32124, 1:1000), anti-Bax (ab32503, 1:2000), anti-cytosolic cytochrome *c* (Cyt *c*) (ab133504, 1:5000), anti-caspase-3 (ab4051, 1:300), anti-cleaved caspase-3 (ab13847, 1:300), and anti-GAPDH (ab9485, 1:2500) were obtained from Abcam Company (Cambridge, UK). Next, the membranes were soaked in TBST buffer with HRP conjugated sheep anti-rabbit secondary antibody (BA1054, 1:1000) obtained from Boster Biological Technology Co. Ltd. (Pleasanton, USA) for 2 h. Densities of protein bands were measured with BandScan 5.0 (Glyko Inc., Novato, CA, USA).

2.10. Statistical analysis

Data were represented as Mean ± SD. We chose one sample Kolmogorov Smirnov test to analyze the normality of data, Levene's test to analyze homogeneity of data, and one-way ANOVA with a LSD test for variance equality or a Dunnett's test for variance inequality by using SPSS 25.0 software (IBM Corp., NY, USA). Group comparisons were statistically remarkable when $p < 0.05$.

3. Results

3.1. Influence of SRG on PC12 cell viability

There were significant deviations in cell viability between groups (One-Sample Kolmogorov-Smirnov test: $P_{(\text{sig 2-tailed})} > 0.05$, the data obey the normal distribution; Levene's test: $F(5,30) = 151.436$, $P_{\text{homogeneity test of variance}} = 0.010$). The viability of PC12 cells in the model group was statistically significant reduction of 56.83 ± 3.46% in comparison with that in the control group (Fig. 2). This suggests that the toxicity of CORT inhibits PC12 cells's proliferation. The viability of PC12 cells in 10 μM BUS group, 5 μM SRG group, 10 μM SRG group, and 20 μM SRG group was statistically significant increase of 78.47 ± 2.91%, 69.11 ± 2.25%, 70.21 ± 2.19%, and 73.45 ± 1.75%, respectively, in comparison with that in the model group (Fig. 2). This suggests that SRG can promote CORT-induced PC12 cells's proliferation in a concentration-dependent way.

3.2. Influence of SRG on LDH leakage from PC12 cells

There were significant deviations in LDH leakage from PC12 cells between groups (One-Sample Kolmogorov-Smirnov test: $P_{(\text{sig 2-tailed})} > 0.05$, the data obey the normal distribution; Levene's test: $F(5,12) = 52.070$, $P_{\text{homogeneity test of variance}} = 0.121$). The LDH leakage value of the model group was more than that of the control group with a statistically significant difference (Fig. 3). This indicates that CORT is cytotoxic to PC12 cells. The LDH leakage value of SRG groups were lower than that of model group with a statistically significant difference

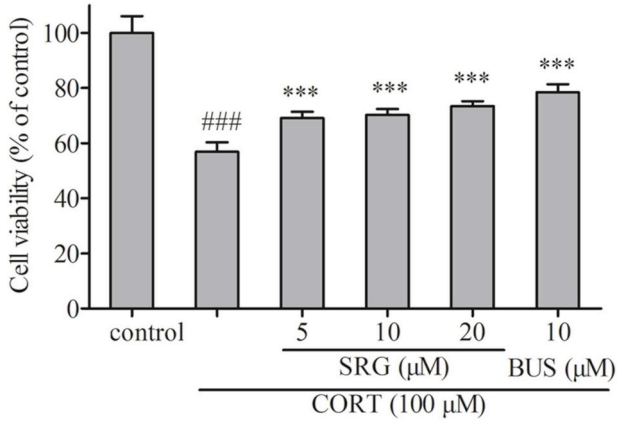

Fig. 2. Influence of SRG on viability of PC12 cells exposed to CORT. Data were in the form of Mean ± SD (n = 6), and results were analyzed by one-way ANOVA with Dunnett's T3 test. ***P < 0.001 compared with the models (CORT); ###P < 0.001 compared with the controls. SRG: (-)-Syringaresinol-4-O-β-D-glucopyranoside; CORT: corticosterone; BUS: buspirone.

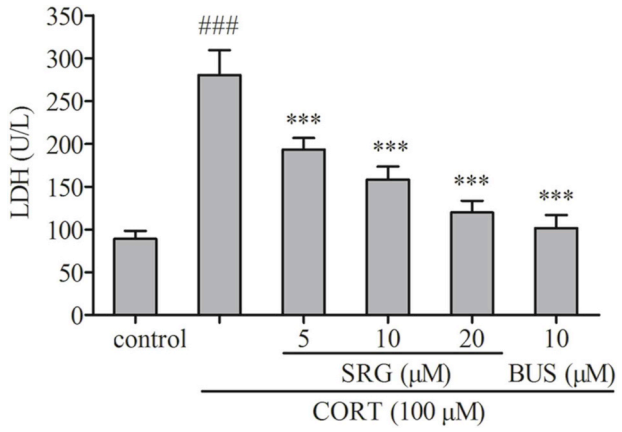

Fig. 3. Influence of SRG on LDH leakage from PC12 cells exposed to CORT. Data were in the form of Mean ± SD (n = 3), and results were analyzed by one-way ANOVA with LSD test. ***P < 0.001 compared with the models (CORT); ###P < 0.001 compared with the controls. SRG: (-)-Syringaresinol-4-O-β-D-glucopyranoside; CORT: corticosterone; BUS: buspirone.

in a concentration dependent manner, and the LDH leakage value of 10 μM BUS group also showed a statistically significant decline in comparison with that of the model group (Fig. 3). This suggests that SRG can reduce CORT-induced damage to PC12 cells.

3.3. Influence of SRG on PC12 cell apoptosis

3.3.1. Flow cytometry analysis with FITC-coupled AV and PI staining

There were significant deviations in the apoptosis of PC12 cells evaluated by flow cytometry analysis between groups (One-Sample Kolmogorov-Smirnov test: $P_{(\text{sig 2-tailed})} > 0.05$, the data obey the normal distribution; Levene's test: F(5,12) = 49.431, $P_{\text{homogeneity test of variance}} = 0.164$, early apoptosis; F(5,12) = 43.343, $P_{\text{homogeneity test of variance}} = 0.046$, late apoptosis; F(5,12) = 281.693, $P_{\text{homogeneity test of variance}} = 0.815$, total apoptosis). The percentage of early apoptotic PC12 cells, late apoptotic PC12 cells, and total apoptotic PC12 cells in the model group were more than that in the control group with a statistically significant difference, respectively (Fig. 4(b)). This indicates that CORT can induce the apoptosis of PC12 cells. The percentage of early apoptotic PC12 cells in the four treatment groups (10 μM BUS group or 5, 10, or 20 μM SRG group) were less than that in the model group with a statistically significant difference, respectively (Fig. 4(b)). The percentage of late apoptotic PC12 cells in 20 μM SRG group and 10 μM BUS group were lower than that in the model group with a statistically significant difference (Fig. 4(b)). The percentage of total apoptotic PC12 cells in SRG groups were lower than that in the model group with a statistically significant difference in a concentration dependent manner, and the percentage of total apoptotic PC12 cells in 10 μM BUS group also showed a statistically significant decline in comparison with that in the model group (Fig. 4(b)). This suggests that SRG can inhibit CORT-induced PC12 cells's apoptosis.

3.3.2. TUNEL assay through nick end labeling of DNA with tetramethylrhodamine-mediated dUTP

There were significant deviations in the apoptosis of PC12 cells evaluated by TUNEL assay between groups (One-Sample Kolmogorov-Smirnov test: $P_{(\text{sig 2-tailed})} > 0.05$, the data obey the normal distribution; Levene's test: F(5,12) = 95.806, $P_{\text{homogeneity test of variance}} = 0.034$). The apoptotic index (AI) value of PC12 cells in the model group was more than that in the control group with a statistically significant difference (Fig. 5(b)). This indicates that CORT can induce the fragmentation of nuclear DNA in PC12 cells during the late stage of apoptosis. The AI values of PC12 cells in 10 μM SRG, 20 μM SRG, and 10 μM BUS group were lower than that in the model group with a statistically significant difference, respectively (Fig. 5(b)). This suggests that SRG can reduce the fragmentation of nuclear DNA in PC12 cells during the late stage of apoptosis.

3.4. Influence of SRG on PC12 cells's ΔΨm

There were significant deviations in the ΔΨm values of PC12 cells as determined by rhodamine 123 staining flow cytometry between groups (One-Sample Kolmogorov-Smirnov test: $P_{(\text{sig 2-tailed})} > 0.05$, the data obey the normal distribution; Levene's test: F(5,12) = 3354.240, $P_{\text{homogeneity test of variance}} = 0.211$). The ΔΨm value of PC12 cells in the model group was less than that in the control group with a statistically significant difference (Fig. 6). This indicates that CORT can cause mitochondrial damage. The ΔΨm values of PC12 cells in SRG groups were more than that in the model group with a statistically significant difference in a concentration dependent manner, and the ΔΨm values of PC12 cells in 10 μM BUS group also showed a statistically significant increase in comparison with that in the model group (Fig. 6). This suggests that SRG can reduce CORT-induced PC12 cells's mitochondrial damage.

3.5. Influence of SRG on PC12 cells's $[Ca^{2+}]_i$

There were significant deviations in PC12 cell $[Ca^{2+}]_i$ between groups (One-Sample Kolmogorov-Smirnov test: $P_{(\text{sig 2-tailed})} > 0.05$, the data obey the normal distribution; Levene's test: F(5,12) = 3100.148, $P_{\text{homogeneity test of variance}} = 0.008$). The PC12 cell $[Ca^{2+}]_i$ of the model group was greater than that of the control group with a statistically significant difference (Fig. 7). This indicates that CORT can cause changes in PC12 cells's calcium homeostasis. The $[Ca^{2+}]_i$ of PC12 cells in SRG groups were less than that in the model group with a statistically significant difference in a concentration dependent manner, and the $[Ca^{2+}]_i$ of PC12 cells in 10 μM BUS group also showed a statistically significant decline in comparison with that of the model group (Fig. 7). This suggests that SRG can correct CORT-induced PC12 cells's intracellular calcium homeostasis imbalance.

3.6. Influence of SRG on CREB and BDNF protein expression in PC12 cells

There were significant deviations in CREB and BDNF protein expression level of PC12 cells between groups (One-Sample Kolmogorov-Smirnov test: $P_{(\text{sig 2-tailed})} > 0.05$, the data obey the normal distribution; Levene's test: F(5,12) = 190.406, $P_{\text{homogeneity test of variance}} = 0.499$, CREB; F(5,12) = 99.515, $P_{\text{homogeneity test of}}$

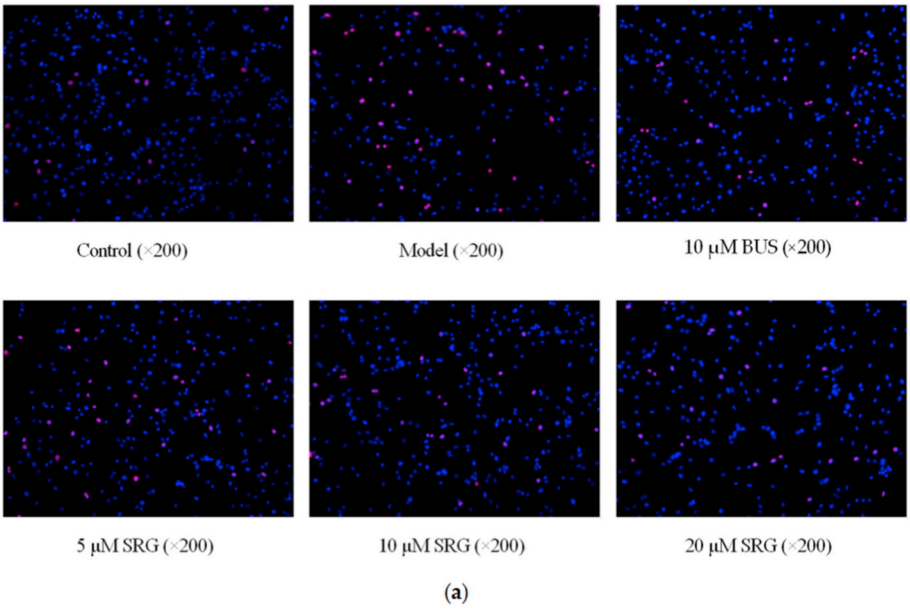

Fig. 4. Influence of SRG on the apoptosis of PC12 cells exposed to CORT by flow cytometry analysis (a) Typical data graph of PC12 cells's apoptosis by flow cytometry analysis with FITC-coupled AV and PI staining; (b) Statistical data chart of PC12 cells's apoptosis plotted in a histogram form. Data were in the form of Mean ± SD (n = 3), and results were analyzed by one-way ANOVA with Dunnett's T3 test (late apoptosis of PC12 cells) and LSD test (early apoptosis and total apoptosis of PC12 cells). $*P < 0.05$, $**P < 0.01$, $***P < 0.001$ compared with the models (CORT); $###P < 0.001$ compared with controls. SRG: (-)-Syringaresinol-4-O-β-D-glucopyranoside; CORT: corticosterone; BUS: buspirone.

$_{\text{variance}}$ = 0.626, BDNF). CREB and BDNF protein expression levels in PC12 cells of the model group were less than those of the control group with a statistically significant difference. Further, CREB and BDNF protein expression levels in PC12 cells of SRG groups were greater than that of the model group with a statistically significant difference in a concentration dependent manner. Meanwhile, CREB and BDNF protein expression levels in PC12 cells of 10 μM BUS group showed a statistically significant increase in comparison with that of the model group (Fig. 8(a) and (b)). This suggests that SRG can increase CORT-induced PC12 cells's CREB and BDNF protein expression levels.

3.7. Influence of SRG on Bax, Cyt c, Bcl-2 protein expression and caspase-3 activity in CORT-induced PC12 cells

There were significant deviations in Bax, Cyt *c*, Bcl-2 protein expression and caspase-3 activity of PC12 cells between groups (One-Sample Kolmogorov-Smirnov test: $P_{(\text{sig 2-tailed})} > 0.05$, the data obey the normal distribution; Levene's test: F(5,12) = 161.206, $P_{\text{homogeneity test of variance}}$ = 0.501, Bax; F(5,12) = 230.539, $P_{\text{homogeneity test of variance}}$ = 0.012, Cyt *c*; F(5,12) = 99.515, $P_{\text{homogeneity test of variance}}$ = 0.028, Bcl-2; F(5,12) = 120.204, $P_{\text{homogeneity test of variance}}$ = 0.021, cleaved caspase-3/caspase-3). Bax and Cyt *c* protein expression levels in PC12 cells of the model group were greater than those of the control group with a statistically significant difference. Further, Bax expression levels in PC12 cells of SRG groups were less than those of the model group with a statistically significant difference in a concentration dependent manner. Cyt *c* protein expression levels in PC12 cells of 10 μM SRG group and 20 μM SRG group were less than those of the model group with a statistically significant difference. Meanwhile, Bax and Cyt *c* protein expression levels in PC12 cells of 10 μM BUS group showed a statistically significant decline in comparison with those of the model group (Fig. 9(a) and (b)). Bcl-2 protein expression levels in PC12 cells of the model group was less than that of the control group with a statistically significant difference. Further, Bcl-2 protein expression levels in PC12 cells of SRG groups were greater than that of the model group with a statistically significant difference in a concentration dependent manner. Meanwhile, Bcl-2 protein expression levels in PC12 cells of 10 μM BUS group showed a statistically significant increase in comparison with that of the model group (Fig. 9(c)). The cleaved caspase-3/caspase-3 ratio represented caspase-3 activity. The caspase-3 activity of PC12 cells in the model group was more than that of the control group with a statistically significant difference. Further, The caspase-3 activity of PC12 cells in the 10 μM BUS group, 10 μM SRG group, and 20 μM SRG group was less than that in the model group with a statistically significant difference, respectively (Fig. 9(d)). This suggests that SRG can up-regulate Bcl-2, down-regulate Bax and Cyt *c* protein expression levels, and reduce caspase-3 activity.

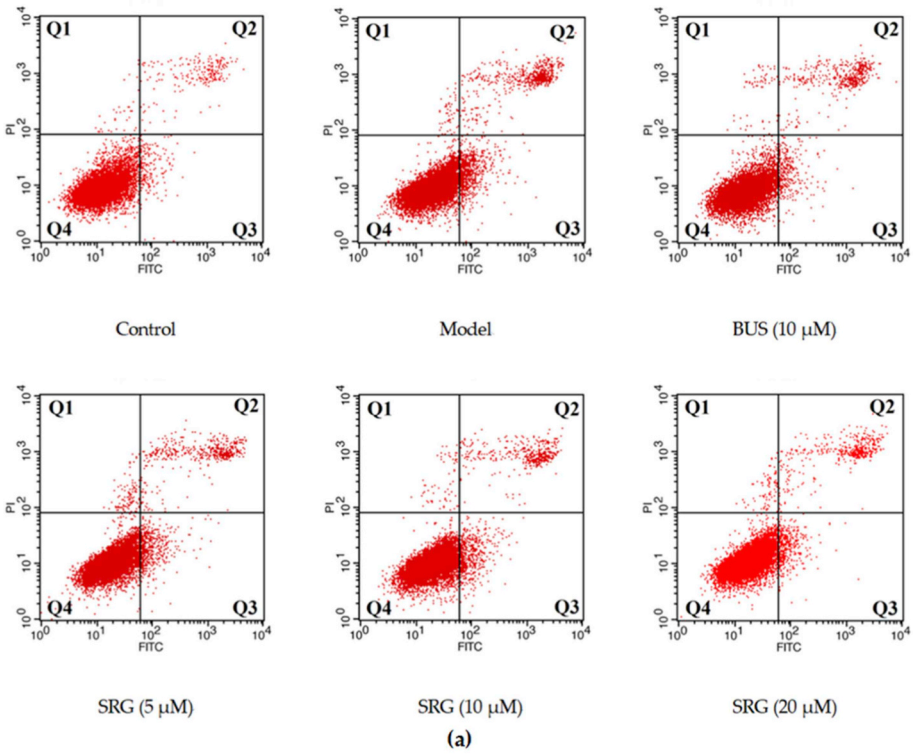

Fig. 5. Influence of SRG on the apoptosis of PC12 cells exposed to CORT by TUNEL assay. (a) Typical fluorescence images of PC12 cell apoptosis by TUNEL assay; (b) Statistical data chart of PC12 cell apoptosis by TUNEL assay plotted in a histogram form. Data were in the form of Mean ± SD (n = 3), and results were analyzed by one-way ANOVA with Dunnett's T3 test. *$P < 0.05$ compared with the models (CORT); #$P < 0.05$ compared with the controls. SRG: (-)-Syringaresinol-4-O-β-D-glucopyranoside; CORT: corticosterone; BUS: buspirone.

4. Discussion

As a pervasive mental illness, anxiety disorder is considered to be the pathological stress response of the body to excessive panic and worry (Elhai et al., 2018; Zhang et al., 2018; Schaefer et al., 2018). In this case, the HPA axis is overactivated, but the negative feedback mechanism of HPA axis adjustment is dysfunctional and sustained high levels of adrenocorticotropin and CORT in the body can cause damage including nerve tissue damage (Goncharova et al., 2019). PC12 cell lines cloned from adult Rattus norvegicus adrenal medulla pheochromocytoma can differentiate into nerve cells under the induction of a nerve cell growth-promoting factor and have remarkable characteristics of cerebral neurons. They were an ideal cell for our in vitro experiment. In this reaserch, we observed SRG's protective effect on neuron damage in the pathogenesis of anxiety disorder by inducing nerve tissue damage in PC12 cells to mimic the damage observed in anxiety disorder using CORT. BUS, a first-line drug currently used in the clinical treatment of anxiety disorder, was selected as the positive control to evaluate the effects of SRG. Our results showed that 100 μM CORT induced PC12 cell damage and reduced the proliferation of PC12 cells through MTT determination and LDH testing. We found that 5, 10, or 20 μM SRG, as well as BUS, could reverse these changes and effectively improve the viability of PC12 cells. This shows that we used the positive anti-anxiety drug BUS to verify the reliability of the CORT-induced neuronal damage

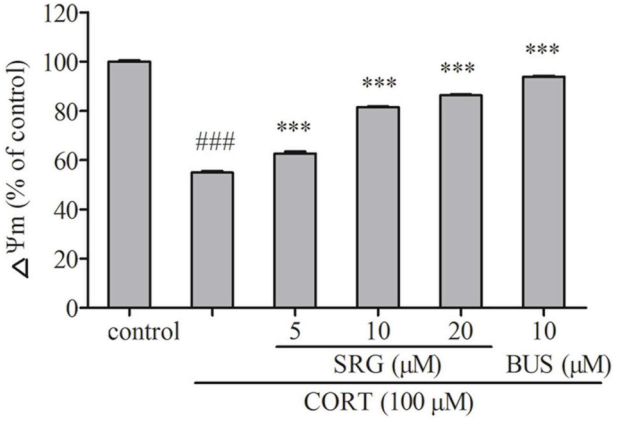

Fig. 6. Influence of SRG on ΔΨm of PC12 cells exposed to CORT. Data were in the form of Mean ± SD (n = 3), and results were analyzed by one-way ANOVA with LSD test. ***P < 0.001 compared with models (CORT); ###P < 0.001 compared with controls. SRG: (-)-Syringaresinol-4-O-β-D-glucopyranoside; CORT: corticosterone; BUS: buspirone.

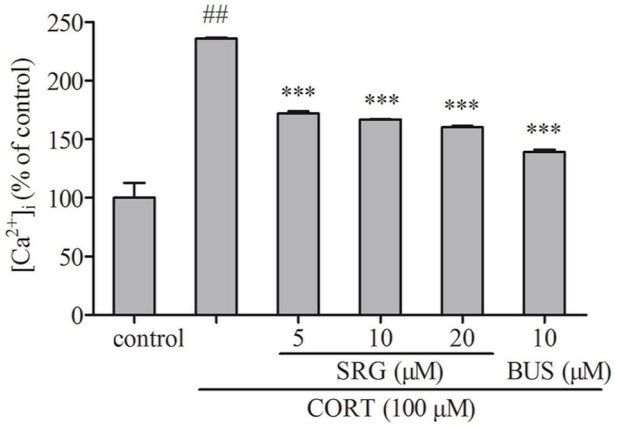

Fig. 7. Influence of SRG on PC12 cell $[Ca^{2+}]_i$ exposed to CORT. Data were in the form of Mean ± SD (n = 3), and results were analyzed by one-way ANOVA with Dunnett's T3 test. ***P < 0.001 compared with the models (CORT); ##P < 0.01 compared with the controls. SRG: (-)-Syringaresinol-4-O-β-D-glucopyranoside; CORT: corticosterone; BUS: buspirone.

model in anxiety disorder, and it also suggests that SRG may play a neuroprotective role in CORT-induced neuronal damage in anxiety disorder. Furthermore, we found that SRG and BUS could activate the pathways involving CREB and BDNF and inhibit the mitochondrial apoptosis pathway, which are pathways related to the pathogenesis of anxiety disorder. This suggests that the anti-anxiety mechanism of SRG is partly the same as that of BUS.

We explored the possible cytoprotective mechanism of SRG in PC12 cells. Apoptosis is a genetically controlled, adjustable, and active cell death process. Changes in cellular morphology during apoptosis involve a multi-stage process. First, cells shrink in size, their connections disappear, and they detach from surrounding cells. Second, cytoplasmic density increases, ΔΨm disappears, permeability changes, and Cyt *c* is released into the cytoplasm with $[Ca^{2+}]_i$ overload. Finally, chromosomal DNA is degraded into about 180–200 bp fragments, and the remains of apoptotic cells are degraded into several apoptotic bodies (Lee et al., 1993). It has been reported that the hippocampal tissue of anxiety model rats exhibits significant apoptosis, and reducing the anxiety-like behavior can reduce the occurrence of apoptosis (Karimi et al., 2014). Studies have further revealed that apoptosis is the main manifestation of CORT-induced damage to PC12 cells and hippocampal cells (Li et al., 2003; Reagan and McEwen, 1997; Crochemore et al., 2005). Thus, neuronal apoptosis may be involved in the pathophysiological mechanism of anxiety disorder. In this research, we found that SRG and BUS decreased the percentage of early apoptotic cells, improved ΔΨm values, decreased $[Ca^{2+}]_i$, and down-regulated Cyt *c* protein expression in PC12 cells during early apoptosis. Further, SRG and BUS decreased the percentage of late apoptotic cells and reduced AI values of PC12 cells during analysis of PC12 cell late apoptosis. Therefore, we determined that SRG and BUS had an anti-apoptotic effect on PC12 cells induced by CORT. In particular, ΔΨm indicates mitochondrial dysfunction and is a characteristic phenomenon of early mitochondrial apoptosis (Lv et al., 2017). The occurrence of mitochondrial apoptosis is an important mechanism leading to mitochondrial dysfunction (Ly et al., 2003). Report suggests that CORT induces mitochondrial apoptosis by decreasing PC12 cell ΔΨm (Liu et al., 2011). Our results showed that SRG and BUS improved the ΔΨm values in a concentration-dependent manner. This suggests that the anti-apoptotic effect of SRG and BUS involve the mitochondrial pathway. Bax (mitochondrial proapoptotic protein) and bcl-2 (mitochondrial antiapoptotic protein) play important roles in mitochondrial apoptosis, and an imbalance between bcl-2 and Bax leads to a decrease in ΔΨm and a change in permeability, thus causing Cyt *c* release from mitochondria to form an inducer that promotes accelerated apoptosis, thereby resulting in the cleavage of caspase-3 into active forms, and eventually, apoptosis (Garrido et al., 2006; Silakhori et al., 2018). In the current study, we found that PC12 cells exposed to CORT had significantly increased Bax and Cyt *c* expression levels, an increased expression ratio of cleaved caspase-3 to caspase-3 proteins, and a decreased Bcl-2 protein expression level. SRG and BUS inhibited CORT-induced apoptosis in PC12 cells by up-regulating Bcl-2 expression,

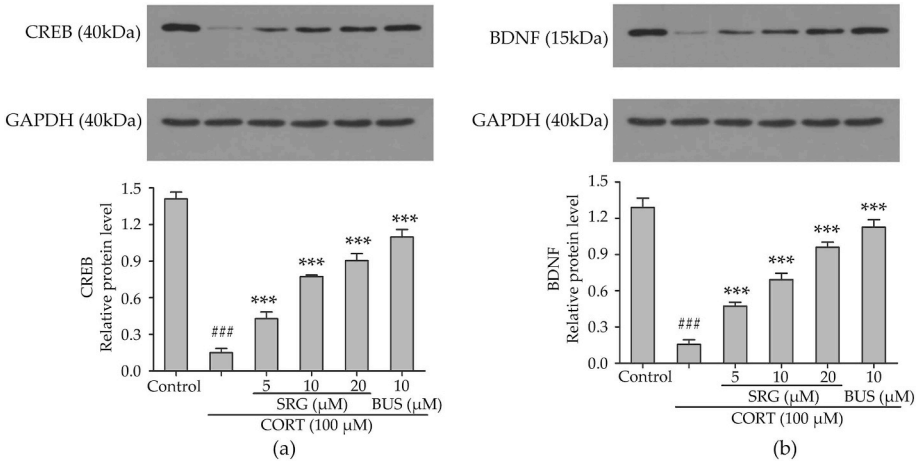

Fig. 8. Influence of SRG on CREB(a) and BDNF(b) protein expression of PC12 cells exposed to CORT. Data were in the form of Mean ± SD (n = 3), and results were analyzed by one-way ANOVA with LSD test. ***P < 0.001 compared with models (CORT); ###P < 0.001 compared with controls. SRG: (-)-Syringaresinol-4-O-β-D-glucopyranoside; CORT: corticosterone; BUS: buspirone.

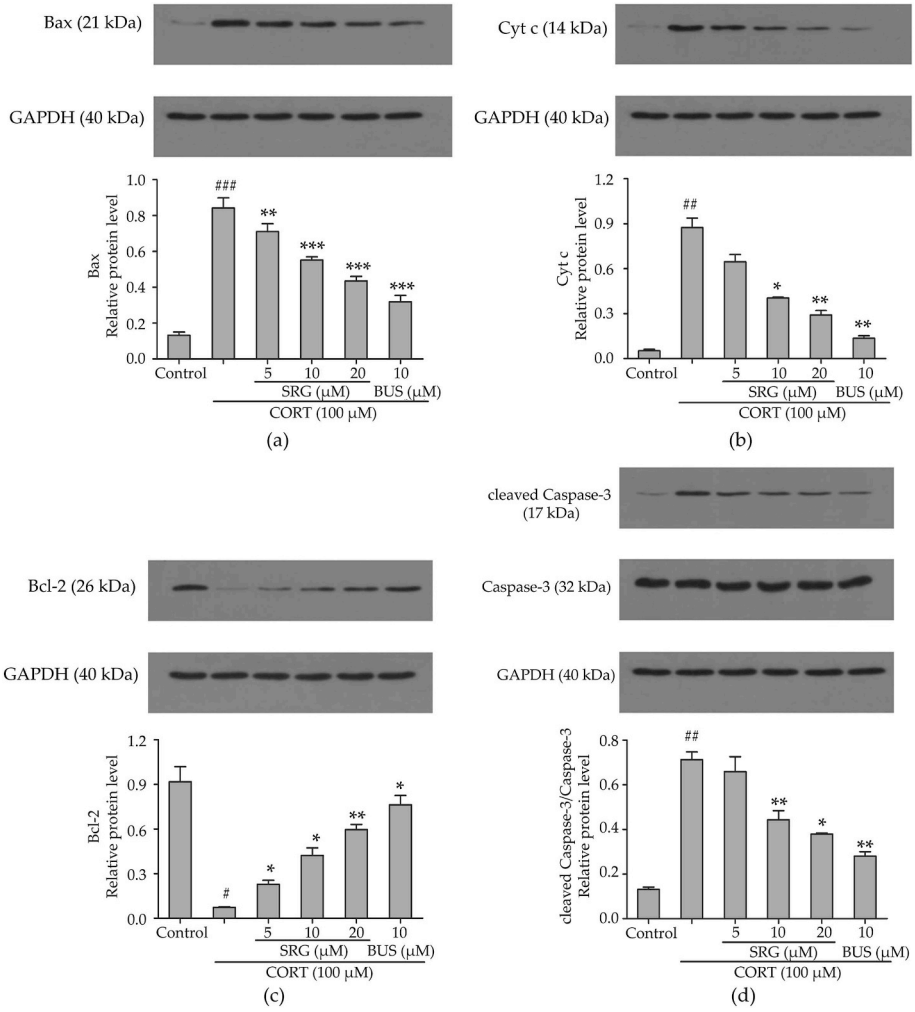

Fig. 9. Influence of SRG on Bax (a), Cyt *c* (b), Bcl-2 (c) protein expression and caspase-3 activity (d) of PC12 cells exposed to CORT. Data were in the form of Mean ± SD (n = 3), and results were analyzed by one-way ANOVA with Dunnett's T3 test (Cyt *c*, Bcl-2 protein expression and caspase-3/caspase-3) and LSD test (Bax protein expression). $^{*}P < 0.05$, $^{**}P < 0.01$, $^{***}P < 0.001$ compared with models (CORT); $\#P < 0.05$, $\#\#P < 0.01$, $\#\#\#P < 0.001$ compared with controls. SRG: (-)-Syringaresinol-4-O-β-D-glucopyranoside; CORT: corticosterone; BUS: buspirone.

down-regulating Bax and Cyt *c* expression, and reducing caspase-3 cleavage into active forms. These results show that the potential mechanisms of SRG and BUS are related to the inhibition of the mitochondrial apoptosis pathway.

CREB, a known transcription enhancer, is a nuclear protein that can bind to cAMP response elements and stimulate gene transcription. CREB activates genes in brain nerve cells that are linked to long-term memory and anxiety formation, including BDNF (Lonze and Ginty, 2002; Du et al., 2019). BDNF has a neurotrophic effect on brain tissue, which is particularly important for nerves damaged during anxiety disorders (Bennett et al., 2016; Yu et al., 2015; Antipova et al., 2009; Li et al., 2010). Studies have shown that CORT and BDNF in brain tissue regulate anxiety behavior in mice (Kikusui et al., 2019). In the signaling pathway composed of CREB and BDNF, BDNF is a downstream signal molecule directly regulated by CREB, and CREB activation could promote BDNF protein expression. Clinical and animal studies have shown that BDNF protein expression level in brain tissue decreases during anxiety disorders, and that anti-anxiety therapy increases both CREB and BDNF protein expression levels (Kim et al., 2008; Ramezany et al., 2019). Studies have shown that BDNF can affect apoptosis by increasing the expression of bcl-2 protein, a key factor in the mitochondrial pathway (Sun et al., 2012). These findings indicate that activating the signaling pathway consisting of CREB and BDNF has a positive effect in anti-anxiety therapy. In our research, we found that PC12 cells exposed to CORT had significantly decreased CREB and BDNF expression levels, SRG and BUS up-regulated both CREB and BDNF expression levels. These results show that the potential mechanisms of SRG and BUS also involve activation of the CREB and BDNF signaling pathway.

Some studies have shown that the extract of Cortex *Albizziae*, a traditional Chinese medicine, has an anti-anxiety effect (Kim et al., 2004; Jung et al., 2005, 2013bib_Jung_et_al_2005bib_Jung_et_al_2013; Liu et al., 2017). To find a better natural anti-anxiety medicine, we conducted detailed research on Cortex *Albizziae*. The main anxiolytic components (S-75) of Cortex *Albizziae* lignans were selected from Cortex *Albizziae* extract using classic anti-anxiety activity evaluation animal models via an elevated cross maze experiment, a light and shade box experiment, and an open field experiment (Tian, 2015). S-75 and its seven main monomer components (including SRG) that could be transferred into the blood (Fan, 2016) acted on corticosterone-damaged PC12 cells and all compounds promoted PC12 cell proliferation. Of these, SRG significantly promoted PC12 cell proliferation, in this case, the dose-activity relationship was obvious and thus, SRG might be the main active anti-anxiety ingredient of Cortex *Albizziae* lignans (Wu, 2017). Based on these previous studies and the data from the current study, we believe that the anti-anxiety effect of Cortex *Albizziae* is partly dependent on the neuroprotective and anti-apoptotic effect of SRG. In addition, SRG is a candidate compound with an anti-anxiety effect that we explored in the anti-anxiety Cortex *Albizziae* study, which is the

main result to be reported in our work. Of course, this study only discusses the in vitro evaluation of SRG's potential anti-anxiety effect. We will confirm this in animal models of anxiety disorders and further explore its mechanism of action related to anti-anxiety disorders.

5. Conclusions

Our study shows that SRG has a neuroprotective and anti-apoptotic effects. We found that the intrinsic mechanism of these effects is partly due to SRG's activation of CREB-BDNF pathway and inhibition of mitochondrial apoptosis pathway. These results provide a valuable preliminary data on SRG's neuroprotective effect on CORT-induced neuronal injury in the pathogenesis of anxiety disorder, and there is a certain reference value for further anti-anxiety studies of this plant drug in the future.

CRediT authorship contribution statement

Desen Yang: Methodology, Data curation, Writing - original draft. **Wanqin Wu:** Methodology, Software, Data curation, Writing - original draft. **Guoping Gan:** Conceptualization, Writing - review & editing. **Dingkun Wang:** Software, Data curation. **Jing Gong:** Data curation. **Ke Fang:** Data curation. **Fuer Lu:** Conceptualization, Writing - review & editing.

Declaration of competing interest

The authors declare that they have no known competing financial interests or personal relationships that could have appeared to influence the work reported in this paper.

Acknowledgements

This research was funded by the National Natural Science Foundation of China (grant number 81274069). We are very much thanks to the Cell Bank of Shanghai institute of life sciences, which provided the rat adrenal pheochromocytoma cell line PC12 cells.

Appendix A. Supplementary data

Supplementary data to this article can be found online at https://doi.org/10.1016/j.fct.2020.111394.

References

Andero, R., Ressler, K.J., 2012. Fear extinction and BDNF: translating animal models of PTSD to the clinic. Gene Brain Behav. 11 (5), 503–512. https://doi.org/10.1111/j.1601-183X.2012.00801.x. PMID: 22530815 PMCID: PMC3389160.

Anderson, D.J., Michelsohn, A., 1989. Role of glucocorticoids in the chromaffin neuron developmental decision. Int. J. Dev. Neurosci. 7 (5), 475–487 PMID: 2816485.

Antipova, T.A., Sapozhnikova, D.S., Bakhtina, Liu, Seredenin, S.B., 2009. Selective anxiolytic afobazole increases the content of BDNF and NGF in cultured hippocampal HT-22 line neurons. Eksp. Klin. Farmakol. 72 (1), 12–14 PMID: 19334503.

Battaglia, M., Ogliari, A., 2005. Anxiety and panic: from human studies to animal research and back. Neurosci. Biobehav. Rev. 29 (1), 169–179. https://doi.org/10.1016/j.neubiorev.2004.06.013. PMID: 15652264.

Bennett, M.R., Hatton, S.N., Lagopoulos, J., 2016. Stress, trauma and PTSD: translational insights into the core synaptic circuitry and its modulation. Brain Struct. Funct. 221 (5), 2401–2426. https://doi.org/10.1007/s00429-015-1056-1. PMID: 25985955.

Carlini, E.A., 2003. Plants and the central nervous system. Pharmacol. Biochem. Behav. 75 (3), 501–512 PMID: 12895668.

Cheng, W., Chen, W., Wang, P., Chu, J., 2018. Asiatic acid protects differentiated PC12 cells from Aβ25-35-induced apoptosis and tau hyperphosphorylation via regulating PI3K/Akt/GSK-3β signaling. Life Sci. 208, 96–101. https://doi.org/10.1016/j.lfs.2018.07.016. PMID: 30017668.

Crochemore, C., Lu, J., Wu, Y., Liposits, Z., Sousa, N., Holsboer, F., Almeida, O.F., 2005. Direct targeting of hippocampal neurons for apoptosis by glucocorticoids is reversible by mineralocorticoid receptor activation. Mol. Psychiatr. 10 (8), 790–798. https://doi.org/10.1038/sj.mp.4001679. PMID: 15940303.

Dobashi, Y., Bhattacharjee, R.N., Toyoshima, K., Akiyama, T., 1996. Upregulation of the APC gene product during neuronal differentiation of rat pheochromocytoma PC12 cells. Biochem. Biophys. Res. Commun. 224 (2), 479–483. https://doi.org/10.1006/bbrc.1996.1052. PMID: 8702414.

Duman, R.S., 2017. BDNF, 5-HT, and anxiety: identification of a critical periadolescent developmental period. Am. J. Psychiatr. 174 (12), 1137–1139. https://doi.org/10.1176/appi.ajp.2017.17101084. PMID: 29191031 PMCID: PMC5818979.

Du, G.T., Ke, X., Meng, G.L., Liu, G.J., Wu, H.Y., Gong, J.H., Qian, X.D., Cheng, J.L., Hong, H., 2018. Telmisartan attenuates hydrogen peroxide-induced apoptosis in differentiated PC12 cells. Metab. Brain Dis. 33 (4), 1327–1334. https://doi.org/10.1007/s11011-018-0237-z. PMID: 29721772.

Du, K., Lu, W., Sun, Y., Feng, J., Wang, J.H., 2019. mRNA and miRNA profiles in the nucleus accumbens are related to fear memory and anxiety induced by physical or psychological stress. J. Psychiatr. Res. 118, 44–65. https://doi.org/10.1016/j.jpsychires.2019.08.013. PMID: 31493709.

Elhai, J.D., Levine, J.C., Hall, B.J., 2018. The relationship between anxiety symptom severity and problematic smartphone use: a review of the literature and conceptual frameworks. J. Anxiety Disord. 62, 45–52. https://doi.org/10.1016/j.janxdis.2018.11.005. PMID: 30529799.

Fan, X.L., 2016 May 30. A Preliminary Study on the Serum Pharmaeochemistry and the Chemical Composition of the Antianxiety Extracts from Cortex *Albizziae*. Master's Thesis. Hubei University of Chinese Medicine, Wuhan, Hubei Province, China.

Garrido, C., Galluzzi, L., Brunet, M., Puig, P.E., Didelot, C., Kroemer, G., 2006. Mechanisms of cytochrome c release from mitochondria. Cell Death Differ. 13 (9), 1423–1433. https://doi.org/10.1038/sj.cdd.4401950. PMID: 16676004.

Goncharova, N., Chigarova, O., Rudenko, N., Oganyan, T., 2019. Glucocorticoid negative feedback in regulation of the hypothalamic-pituitary-adrenal axis in Rhesus monkeys with various types of adaptive behavior: individual and age-related differences. Front. Endocrinol. 10, 24. https://doi.org/10.3389/fendo.2019.00024. PMID: 30814974 PMCID: PMC6381009.

Hempstead, B.L., 2015. Brain-derived neurotrophic factor: three ligands, many actions. Trans. Am. Clin. Climatol. Assoc. 126, 9–19 PMID: 26330656 PMCID: PMC4530710.

Ji, L.L., Peng, J.B., Fu, C.H., Tong, L., Wang, Z.Y., 2017. Sigma-1 receptor activation ameliorates anxiety-like behavior through NR2A-CREB-BDNF signaling pathway in a rat model submitted to single-prolonged stress. Mol. Med. Rep. 16 (4), 4987–4993. https://doi.org/10.3892/mmr.2017.7185. PMID: 28791385.

Jiang, B.P., Liu, Y.M., Le, L., Li, Z.Y., Si, J.Y., Liu, X.M., Chang, Q., Pan, R.L., 2014. Cajaninstilbene acid prevents corticosterone-induced apoptosis in PC12 cells by inhibiting the mitochondrial apoptotic pathway. Cell. Physiol. Biochem. 34 (3), 1015–1026. https://doi.org/10.1159/000366317. PMID: 25199566.

Jung, J.W., Cho, J.H., Ahn, N.Y., Oh, H.R., Kim, S.Y., Jang, C.G., Ryu, J.H., 2005. Effect of chronic *Albizzia julibrissin* treatment on 5-hydroxytryptamine 1A receptors in rat brain. Pharmacol. Biochem. Behav. 81 (1), 205–210. https://doi.org/10.1016/j.pbb.2005.03.014. PMID:15894080.

Jung, Y.H., Ha, R.R., Kwon, S.H., Hong, S.I., Lee, K.H., Kim, S.Y., Lee, S.Y., Jang, C.G., 2013. Anxiolytic effects of Julibroside C1 isolated from *Albizzia julibrissin* in mice. Prog. Neuro-Psychopharmacol. Biol. Psychiatry 44, 184–192. https://doi.org/10.1016/j.pnpbp.2013.02.012. PMID: 23481219.

Karimi, S., Jahanshahi, M., Golalipour, M.J., 2014. The effect of MDMA-induced anxiety on neuronal apoptosis in adult male rats' hippocampus. Folia Biol. 60 (4), 187–191 PMID: 25152052.

Kikusui, T., Kanbara, N., Ozaki, M., Hirayama, N., Ida, K., Tokita, M., Tanabe, N., Mitsuyama, K., Abe, H., Yoshida, M., Nagasawa, M., Mogi, K., 2019. Early weaning increases anxiety via brain-derived neurotrophic factorsignaling in the mouse prefrontal cortex. Sci. Rep. 9 (1), 3991. https://doi.org/10.1038/s41598-019-40530-9. PMID: 30850750 PMCID: PMC6408497.

Kim, B., Kim, C.Y., Hong, J.P., Kim, S.Y., Lee, C., Joo, Y.H., 2008. Brain-derived neurotrophic factor Val/Met polymorphism and bipolar disorder. Association of the Met allele with suicidal behavior of bipolar patients. Neuropsychobiology 58, 97–103. https://doi.org/10.1159/000162356. PMID: 18843195.

Kim, W.K., Jung, J.W., Ahn, N.Y., Oh, H.R., Lee, B.K., Oh, J.K., 2004. Anxiolytic-like effects of extracts from *Albizzia julibrissin* bark in the elevated plus-maze in rats. Life Sci. 75 (23), 2787–2795. https://doi.org/10.1016/j.lfs.2004.05.024. PMID: 15464830.

Lader, M., Morton, S., 1991. Benzodiazepine problems. Br. J. Addict. 86 (7), 823–828 PMID: 1680514.

Lang, S.B., Stein, V., Bonhoeffer, T., Lohmann, C., 2007. Endogenous brain-derived neurotrophic factor triggers fast calcium transients at synapses in developing dendrites. J. Neurosci. 27 (5), 1097–1105. https://doi.org/10.1523/JNEUROSCI.3590-06.2007. PMID: 17267564PMID.

Lee, S., Christakos, S., Small, M.B., 1993. Apoptosis and signal transduction: clues to a molecular mechanism. Curr. Opin. Cell Biol. 5 (2), 286–291. https://doi.org/10.1016/0955-0674(93)90118-a. PMID: 8507500.

Levada, O.A., Cherednichenko, N.V., 2015. Brain-derived neurotrophic factor (BDNF): neurobiology and marker value in neuropsychiatry. Lik Sprava (3–4), 15–25 PMID: 26827434.

Li, Q., Qu, F.L., Gao, Y., Jiang, Y.P., Rahman, K., Lee, K.H., Han, T., Qin, L.P., 2017. *Piper sarmentosum* Roxb. produces antidepressant-like effects in rodents, associated with activation of the CREB-BDNF-ERK signaling pathway and reversal of HPA axis hyperactivity. J. Ethnopharmacol. 199, 9–19. https://doi.org/10.1016/j.jep.2017.01.037. PMID: 28126450.

Li, Y.F., Gong, Z.H., Yang, M., Zhao, Y.M., Luo, Z.P., 2003. Inhibition of the oligosaccharides extracted from *Morinda officinalis*, a Chinese traditional herbal medicine, on the corticosterone induced apoptosis in PC12 cells. Life Sci. 72 (8), 933–942 PMID: 12493574.

Li, Y.F., Liu, Y.Q., Yang, M., Wang, H.L., Huang, W.C., Zhao, Y.M., Luo, Z.P., 2004. The cytoprotective effect of inulin-type hexasaccharide extracted from Morinda officinalis on PC12 cells against the lesion induced by corticosterone. Life Sci. 75 (13),

1531–1538. https://doi.org/10.1016/j.lfs.2004.02.029. PMID: 15261759.
Li, W.J., Yu, H., Yang, J.M., Gao, J., Jiang, H., Feng, M., Zhao, Y.X., Chen, Z.Y., 2010. Anxiolytic effect of music exposure on BDNFMet/Met transgenic mice. Brain Res. 1347, 71–79. https://doi.org/10.1016/j.brainres.2010.05.080. PMID: 20515664.
Li, Y.F., Yang, M., Zhao, Y.M., Luan, X.H., Luo, Z.P., 2002. Antagonistic effect of aqueous extract of detoxified cottonseeds on corticosterone-induced lesion in cultured PC12 cells. Zhongguo Zhongyao Zazhi 27 (6), 442–446 PMID: 12774637.
Li, Z.Y., Li, Q.Z., Chen, L., Chen, B.D., Zhang, C., Wang, X., Li, W.P., 2016. HPOB, an HDAC6 inhibitor, attenuates corticosterone-induced injury in rat adrenal pheochromocytoma PC12 cells by inhibiting mitochondrial GR translocation and the intrinsic apoptosis pathway. Neurochem. Int. 99, 239–251. https://doi.org/10.1016/j.neuint.2016.08.004. PMID: 27522966.
Liu, B., Zhang, H., Xu, C., Yang, G., Tao, J., Huang, J., Wu, J., Duan, X., Cao, Y., Dong, J., 2011. Neuroprotective effects of icariin on corticosterone-induced apoptosis in primary cultured rat hippocampal neurons. Brain Res. 1375, 59–67. https://doi.org/10.1016/j.brainres.2010.12.053. PMID: 21182828.
Liu, J., Lv, Y.W., Shi, J.L., Ma, X.J., Chen, Y., Zheng, Z.Q., Wang, S.N., Guo, J.Y., 2017. Anti-anxiety effect of (-)-syringaresnol-4-O-β-d-apiofuranosyl-(1→2)-β-d-glucopyranoside from *Albizzia julibrissin* Durazz. (Leguminosae). pii: E1331. Molecules 22 (8). https://doi.org/10.3390/molecules22081331. PMID: 28800105.
Lonze, B.E., Ginty, D.D., 2002. Function and regulation of CREB family transcription factors in the nervous system. Neuron 35 (4), 605–623 PMID: 12194863.
Lv, R., Du, L., Lu, C., Wu, J., Ding, M., Wang, C., Mao, N., Shi, Z., 2017. Allicin protects against H_2O_2-induced apoptosis of PC12 cells via the mitochondrial pathway. Exp Ther Med 14 (3), 2053–2059. https://doi.org/10.3892/etm.2017.4725. PMID: 28962124 PMCID: PMC5609123.
Ly, J.D., Grubb, D.R., Lawen, A., 2003. The mitochondrial membrane potential (deltapsi (m)) in apoptosis; an update. Apoptosis 8 (2), 115–128 PMID: 12766472.
Mohammad Alizadeh, E., Mahdavi, M., Jenani Fard, F., Chamani, S., Farajdokht, F., Karimi, P., 2018. Metformin protects PC12 cells against oxygen-glucose deprivation/reperfusion injury. Toxicol. Mech. Methods 28 (8), 622–629. https://doi.org/10.1080/15376516.2018.1486495. PMID: 29877750.
Mohammadi, A., Amooeian, V.G., Rashidi, E., 2018. Dysfunction in brain-derived neurotrophic factor signaling pathway and susceptibility to schizophrenia, Parkinson's, and Alzheimer's diseases. Curr. Gene Ther. 18 (1), 45–63. https://doi.org/10.2174/1566523218666180302163029. PMID: 29512462.
Nash, J.R., Nutt, D.J., 2005. Pharmacotherapy of anxiety. Handb. Exp. Pharmacol. (169), 469–501 PMID: 16594269.
Peng, C.H., Chiou, S.H., Chen, S.J., Chou, Y.C., Ku, H.H., Cheng, C.K., Yen, C.J., Tsai, T.H., Chang, Y.L., Kao, C.L., 2008. Neuroprotection by imipramine against lipopolysaccharide-induced apoptosis in hippocampus-derived neural stem cells mediated by activation of BDNF and the MAPK pathway. Eur. Neuropsychopharmacol 18 (2), 128–140. https://doi.org/10.1016/j.euroneuro.2007.05.002. PMID: 17566715.
Ramezany, Yasuj S., Nourhashemi, M., Keshavarzi, S., Motaghinejad, M., Motevalian, M., 2019. Possible role of cyclic AMP response element binding/brain-derived neurotrophic factor signaling pathway in mediating the pharmacological effects of duloxetine against methamphetamine use-induced cognitive impairment and withdrawal-induced anxiety and depression in rats. Adv. Biomed. Res. 8, 11. https://doi.org/10.4103/abr.abr_34_18. PMID: 30993081 PMCID: PMC6425746.
Reagan, L.P., McEwen, B.S., 1997. Controversies surrounding glucocorticoid-mediated cell death in the hippocampus. J. Chem. Neuroanat. 13 (3), 149–167 PMID: 9315966.
Schaefer, L.M., Howell, K.H., Thurston, I.B., Kaufman, C.C., Hasselle, A.J., 2018. Protective factors associated with fewer generalized anxiety disorder symptoms among women exposed to intimate partner violence. 886260518817027. J. Interpers Violence. https://doi.org/10.1177/0886260518817027. PMID: 30526241.
Seckl, J.R., Meaney, M.J., 2004. Glucocorticoid programming. Ann. N. Y. Acad. Sci. 1032, 63–84. https://doi.org/10.1196/annals.1314.006. PMID: 15677396.
Seo, J., Maeng, J., Kim, H.J., 2016. Translationally controlled tumor protein stimulates dopamine release from PC12 cells via Ca^{2+}-independent phospholipase A_2 pathways. pii: E1774. Int. J. Mol. Sci. 17 (10). https://doi.org/10.3390/ijms17101774. PMID: 27783042 PMCID: PMC5085798.
Silakhori, S., Hosseinzadeh, H., Shaebani Behbahani, F., Mehri, S., 2018. Neuroprotective effect of clavulanic acid on trimethyltin (TMT)-induced cytotoxicity in PC12 cells. Drug Chem. Toxicol. 15 (2), 1–7. https://doi.org/10.1080/01480545.2018.1468772. PMID: 29764237.
Sun, Z., Ma, X., Yang, H., Zhao, J., Zhang, J., 2012. Brain-derived neurotrophic factor prevents beta- amyloid-induced apoptosis of pheochromocytoma cells by regulating Bax/Bcl-2 expression. Neural Regen Res 7 (5), 347–351. https://doi.org/10.3969/j.issn.1673-5374.2012.05.004. PMID: 25774173 PMCID: PMC4350116.
Tian, W., 2015 May 28. Study on Anxiolytic Effects of the Extracts from Cortex *Albizziae* by Screening and the Influence of Neurotransmitters in the Brain after Chemotherapy. Master's Thesis. Hubei University of Chinese Medicine, Wuhan, Hubei Province, China.
Tong, W., Mi, L., Liang, H., Zhao, Y., 2003. Isolation and identification of chemical constituents from *Albizia julibrissin* Durazz. Beijing Da Xue Xue Bao Yi Xue Ban 35 (2), 180–183 PMID: 12920839.
Wu, W.Q., 2017 May 30. Study on the Mechanism of the Anxiolytic Extracts of Cortex *Albizziae* and the Effect of the Main Active Ingredient on PC12 Cell Apoptosis. Master's Thesis. Hubei University of Chinese Medicine, Wuhan, Hubei Province, China.
Yin, W.L., He, J.Q., Hu, B., Jiang, Z.S., Tang, X.Q., 2009. Hydrogen sulfide inhibits MPP (+)-induced apoptosis in PC12 cells. Life Sci. 85 (7–8), 269–275. https://doi.org/10.1016/j.lfs.2009.05.023. PMID: 19540852.
Yu, D.H., Qiao, S.Y., Zhao, Y.M., 2004. Advances in study on bark of *Albizzia julibrissin*. Zhongguo Zhongyao Zazhi 29 (7), 619–624 PMID: 15503760.
Yu, Y., Wu, S., Li, J., Wang, R., Xie, X., Yu, X., Pan, J., Xu, Y., Zheng, L., 2015. The effect of curcumin on the brain-gut axis in rat model of irritable bowel syndrome: involvement of 5-HT-dependent signaling. Metab. Brain Dis. 30 (1), 47–55. https://doi.org/10.1007/s11011-014-9554-z. PMID: 24807589.
Zhu, M.Y., Wang, W.P., Bissette, G., 2006. Neuroprotective effects of agmatine against cell damage caused by glucocorticoids in cultured rat hippocampal neurons. Neuroscience 141 (4), 2019–2027. https://doi.org/10.1016/j.neuroscience.2006.05.011. PMID: 1677734 PMCID: PMC2921983.
Zhang, J., Liu, X., Fang, L., 2018. Combined effects of depression and anxiety on suicide: a case-control psychological autopsy study in rural China. Psychiatr. Res. 271, 370–373. https://doi.org/10.1016/j.psychres.2018.11.010. PMID: 30529321.
Zheng, L., Wu, G., Wang, B., Wu, L.J., Zhao, Y.Y., 2004. Isolation and identification of chemical constituents from *Albizia julibrissin* Durazz. Beijing Da Xue Xue Bao Yi Xue Ban 36 (4), 421–425 PMID: 15303140.
Zhu, Z.H., Yang, R., Fu, X., Wang, Y.Q., Wu, G.C., 2006. Astrocyte-conditioned medium protecting hippocampal neurons in primary cultures against corticosterone-induced damages via PI3-K/Akt signal pathway. Brain Res. 1114 (1), 1–10. https://doi.org/10.1016/j.brainres.2006.07.070. PMID: 16930567.